The current issue and full text archive of this journal is available at
www.emeraldinsight.com/0961-5539.htm

Wavelet application for reduction of measurement noise effects in inverse boundary heat conduction problems

H. Ahmadi-Noubari
Department of Electrical and Computer Engineering, Faculty of Engineering, University of Tehran, Tehran, Iran, and
A. Pourshaghaghy, F. Kowsary and A. Hakkaki-Fard
Department of Mechanical Engineering, Faculty of Engineering, University of Tehran, Tehran, Iran

Received 15 May 2005
Revised 15 March 2007
Accepted 15 March 2007

Abstract

Purpose – The purpose of this paper is to reduce the destructive effects of existing unavoidable noises contaminating temperature data in inverse heat conduction problems (IHCP) utilizing the wavelets.

Design/methodology/approach – For noise reduction, sensor data were treated as input to the filter bank used for signal decomposition and implementation of discrete wavelet transform. This is followed by the application of wavelet denoising algorithm that is applied on the wavelet coefficients of signal components at different resolution levels. Both noisy and de-noised measurement temperatures are then used as input data to a numerical experiment of IHCP. The inverse problem deals with an estimation of unknown surface heat flux in a 2D slab and is solved by the variable metric method.

Findings – Comparison of estimated heat fluxes obtained using denoised data with those using original sensor data indicates that noise reduction by wavelet has a potential to be a powerful tool for improvement of IHCP results.

Originality/value – Noise reduction using wavelets, while it can be implemented very easily, may also significantly relegate (or even eliminate) conventional regularization schemes commonly used in IHCP.

Keywords Waveforms, Heat conduction

Paper type Research paper

Nomenclature

A = amplitude of the noise
e_{RMS} = relative root mean square error, equation (23)
f = function of sum of squares errors, equation (18)
g = high pass filter of decomposition stage
$\tilde{g}$ = high pass filter of synthesis stage
h = low pass filter of decomposition stage
$\tilde{h}$ = low pass filter of synthesis stage
K = number of sensors
k = conductivity coefficient (W/m^2)
M = total number of time steps
n = total number of unknowns that should be estimated
n_s = number of spatial components of flux
q = heat flux (W/m^2)
$\vec{q}$ = unknown heat flux vector (design vector with dimension $n \times 1$), equation (15)
S = signal

International Journal of Numerical Methods for Heat & Fluid Flow
Vol. 18 No. 2, 2008
pp. 217-236

0961-5539
DOI 10.1108/09615530810846356

T = temperature calculated by the model (K)
t = time (sec)
th = the threshold
X = pulse sensitivity coefficient ($K\,m^2/W$) defined by equation (16)
Y = temperature measured by sensors
(x, y) = Cartesian coordinate system

Greek
α = thermal diffusivity (m^2/sec)
ε = tolerance error
φ = scaling function
ψ = wavelet function
ω = frequency

Superscripts
T = matrix transpose symbol
n_s = total number of spatial components of heat flux
$\tilde{n}$ = index of spatial component of flux ($\tilde{n} = 1, 2, \ldots, n_s$)
$\rightarrow$ = vector

Subscripts
K = sensor index number
M = total number of time steps
$m, \tilde{m}$ = indices of time step, each between 1, 2, ... M

1. Introduction

Inverse heat conduction problems (IHCP), unlike the problems dealing with direct heat conduction, are mathematically ill-posed; being highly sensitive to random errors (noises) that inherently exist in measured temperature data. Therefore, reduction of sensitivity of IHCP methods to these random errors is of critical importance. Methods of IHCP are classified into two categories: sequential methods and whole domain methods. Each of these two types of IHCP methods uses its own remedy to reduce effects of measurement random errors on the estimated results. These remedies are generally referred to as "regularization" techniques.

Sequential function specification (SFS) method is considered as the main approach in the sequential category. A review of SFS and other sequential methods can be found in reference book by Beck *et al.* (1985). Assumption of constant heat fluxes in "r" future time steps in the SFS method has a regularization essence and sometimes is called future times regularization (Woodbury, 2003). This type of regularization introduces bias into the estimation but significantly stabilizes the estimation procedure. Additional comments on this type of regularization can be found in Chapter 2 of the book by Woodbury (2003).

Whole domain IHCP methods act through an iterative process to reach final solution. These methods utilize a non-linear optimization technique as a tool for minimizing the sum of squares of errors function (the objective function). These techniques are generally divided into "discrete type" and "gradient-based" groups. The latter requires the gradient of the objective function while the former does not. The most famous of the first group is the Powell method or the evolutionary genetic algorithm method. In the gradient-based techniques, starting from an initial arbitrary value for the unknowns and using gradient of objective function, the progress is made towards the minimum value of the objective function. The whole domain methods can be regularized for example, by Tikhonov regularization approach in which an additional term is added to the sum of squares function to penalize undesirable variations in the estimated results (Woodbury, 2003, Chapter 2).

The iterative regularization is an alternative technique within the whole domain IHCP types to reduce the sensitivity of inverse problem to noise errors without changing the sum of squares errors function. The main idea in iterative regularization method is to stop the iterative procedure sufficiently close but not very near to the final optimum point. Then with accepting a bias error due to near optimality of the solution, it highly

dampens propagation of noise errors into the estimated solution. Stopping criteria for iterative process of whole domain IHCP based on iterative regularization is determined by what is known as the "discrepancy principle" (Ozisic and Orlande, 2000).

It should be noted that the regularization techniques manipulate the original noisy data and use them "as are" for estimation of unknowns. Some authors have proposed to pre-process the data obtained from the sensors before the IHCP algorithm is applied to them. This approach consists of different digital filtering methods. Al-Khalidy (1998) used digital filter formulation to smooth noisy sensor data in parabolic and hyperbolic inverse heat conduction. In this method, each data value is replaced by a combination of itself and a number of adjacent data. The method is simple for computer programming and is based on a least square approximation. Beck *et al.* (1985, p. 153) proposed a prefiltering formula much simpler than that used by Al-Khalidy in which every data is replaced by $y_m = (Y_{m-1} + 2Y_m + Y_{m+1})/4$ where m is index of time step. Kalman (1960) introduced a filtering technique referred to as Kalman filtering. This technique has been used by some authors to solve IHCP's. Ji and Jang (1998) applied Kalman filter to a one dimensional problem with errors in the measured temperatures by comparing the calculated heat transfer with those obtained experimentally. Tuan *et al.* (1996) and Tuan and Ju (2000) used Kalman filter and a real time least squares algorithm to solve a 2D IHCP.

In this paper, an alternative approach based on wavelet transform, is introduced to modify the sensor data before they are used by IHCP methods. Wavelets, as an alternative approach for data analysis, have been utilized successfully for signal separation and noise reduction (Strang and Nguyen, 1996). In this approach, discrete wavelet transform (DWT) is used to decompose the signal acquired from each sensor in a multi-resolution filter bank structure. Wavelets denoising algorithm is then applied for noise reduction that modifies wavelet coefficients derived during wavelet decomposition. The reconstruction phase is applied to the modified coefficients in order to recover noise reduced signal. The denoised signal is then considered as an input to the inverse algorithm. In the next section, a brief review of wavelets is presented. This is then followed by discussion of noise reduction by wavelets. In Section 4, an inverse problem is defined to be solved by the variable metric method (VMM) using sensor data modified by wavelets. In Section 5, a comparison is made among results of inverse method for three different cases, i.e. those obtained from: noisy data, iterative regularization and the data modified by wavelets.

2. An overview of wavelets and wavelet transform

In the following, a brief review of wavelets and their primary features relevant to this work is given. Comprehensive discussion on the subject can be found in numerous textbooks and review papers written on wavelets. They provide excellent reference material to study the subject (for instance, Strang and Nguyen, 1996; Burrus *et al.*, 1997).

Wavelets are classes of functions with properties that are considered highly suitable for analysis of wide spectrum of signals found in engineering and scientific applications. Wavelets have been applied in communications, data compression, pattern recognition, system modeling and control to name a few. Wavelets are used as basis functions for signal decomposition and reconstruction described briefly as follows.

For a scalar function $\psi(t) : R \rightarrow R$ to be treated as a wavelet it is necessary that $\psi(t)$ satisfy the following conditions:

- to have a finite two norm, i.e. $\int_{-\infty}^{\infty} |\psi(t)|^2 \mathrm{d}t < \infty$;
- to have a finite support width (actual or effective) both in time and frequency domain (to be band limited); and
- to satisfy the admissibility condition defined as:

$$\int_{-\infty}^{\infty} \frac{|\hat{\Psi}(\omega)|^2}{|\omega|} \mathrm{d}\omega < \infty \tag{1}$$

where, $\hat{\Psi}(\omega)$ is the Fourier transform of $\psi(t)$. Admissibility condition refers to behavior of $\hat{\Psi}(\omega)$ near the origin where it is required to approach zero faster than frequency variable ω. The admissibility condition implies $\psi(t)$ to have a zero DC (average) value, i.e. $\int_{-\infty}^{\infty} \psi(t) \mathrm{d}t = 0$.

Figure 1 shows examples of wavelet functions. Wavelets assume different forms; they can be symmetric or asymmetric. Some are expressed analytically; however, most

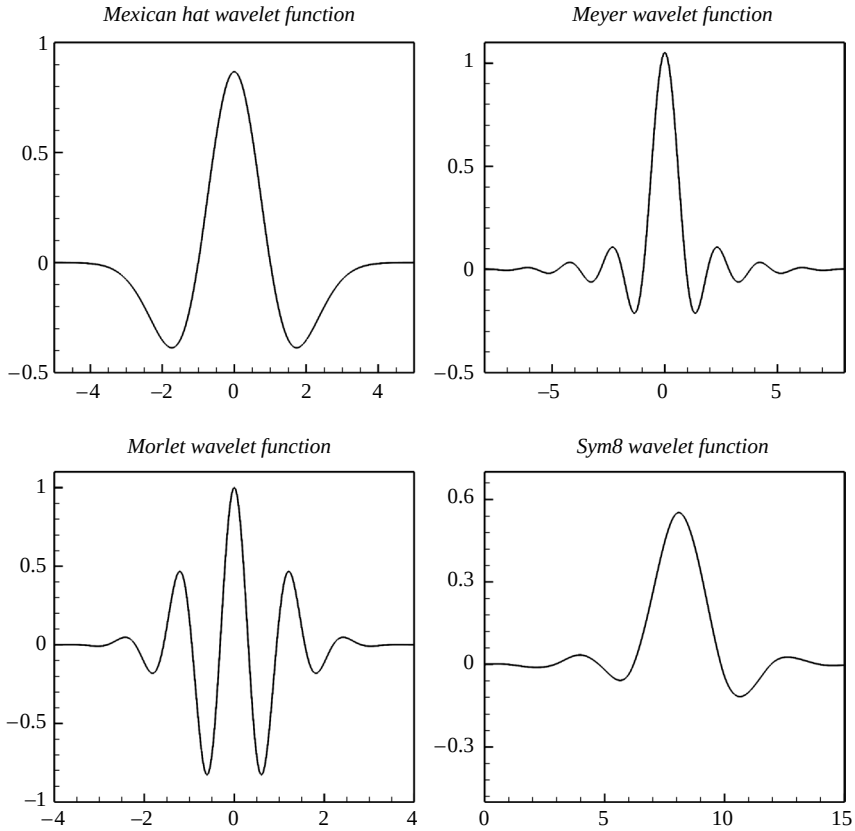

Figure 1.
Examples of wavelet functions

of them are expressed numerically. Wavelets can be complex or real functions, some are infinitely differentiable such as Mexican hat while others have regularity of finite order.

Wavelet transform of a function $f(t) \in L^2$ is defined as follows:

$$W_{a,b} = \int_{-\infty}^{\infty} f(t)\psi\left(\frac{t-b}{a}\right)\mathrm{d}t \tag{2}$$

where scalars a and b are referred to as scale and translation factors, respectively, and $a \neq 0$. The function $\psi((t-b)/a)$ is scaled and translated version of $\psi(t)$ referred to as prototype wavelet. When a, b assume continuous values, equation (2) defines continuous wavelet transform of $f(t)$. Now, let scaling and translation parameters a, b assume the following discrete values:

$$\begin{cases} a = 2^{-j} \\ b = k2^{-j} \end{cases}; \quad j,k \in Z \tag{3}$$

Then translated and scaled version of $\psi(t)$ can be written as:

$$\psi_{jk}(t) = 2^{j/2}\psi(2^j t - k); \quad j,k \in Z \tag{4}$$

$\psi_{jk}(t)$; j, $k \in Z$ constitute a family of wavelet functions constructed from a prototype of wavelet function $\psi(t)$. They are utilized as basis functions for function (signal) expansion. Signal expansion using discrete values of a and b of equation (3) is referred to as DWT. Analysis of a given data in wavelet transform consists of three main stages:

(1) decomposition;

(2) analysis; and

(3) reconstruction (Figure 2).

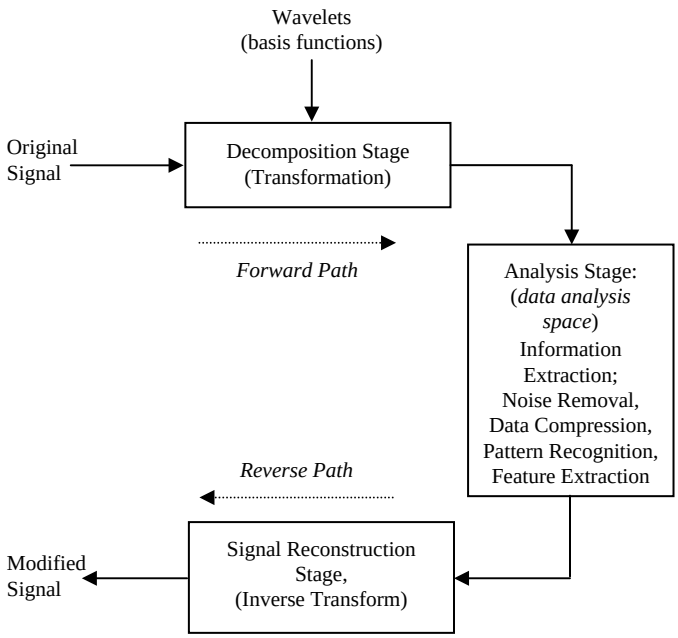

Figure 2.
Main stages in signal processing

2.1 Decomposition stage

In decomposition stage as used in DWT, a given signal is decomposed into a set of low- and high frequency components in a multi resolution structure using filter bank architecture as shown in Figure 3. Decomposition of a signal into a set of hierarchically low- and high frequency components was proposed first by Mallat (1989). In this structure, signal decomposition is carried out by successive filtering of a given signal using low- and high pass filters followed by down sampling by two at each stage as depicted by block diagram in Figure 3 for a three level decomposition. This implementation of DWT is recognized as MRFB structure. Down sampling by two, ⊕, results in deleting signal odd samples. In this representation, $h(k)$'s are the coefficients of low pass filter retaining all low frequency contents of a signal. $g(k)$'s are the coefficients of high pass filters allowing to pass all high frequency components of the signal. a_i's are referred to as "approximations" and d_i are called as "details". In signal expansion as shown in Figure 3, wavelets constitute the basis functions by which signal components a_i and d_i are derived. Furthermore, filter coefficients $h(k)$ and $g(k)$ are directly related to a particular wavelet functions used for a given signal decomposition. In a standard dyadic decomposition of DWT, filter coefficients remain unchanged at all stages (scales) of decomposition. However, in multi-wavelet analysis, different filters are used at different stages. For a complete discussion on the subject and detailed mathematical relations of $h(k)$, $g(k)$, a_i's and d_i's, the reader should refer to the books by Strang and Nguyen (1996) or Burrus *et al.* (1997).

2.2 Analysis and signal manipulation stage

This stage of wavelet analysis of a signal includes the manipulation and coding of wavelet coefficients such as for noise reduction, information extraction, data compression, data transmission. Thresholding of wavelet coefficients is a commonly used form of manipulation of coefficients for noise reduction.

2.3 Synthesis stage

Finally, synthesis stage refers to signal reconstruction where in reverse transformation is applied on the manipulated (modified) coefficients. Manipulation of coefficients results in a set of modified values for coefficients used during reconstruction (synthesis) stage of the signal. For a three level decomposition of Figure 3, synthesis stage also consists of three levels as shown in Figure 4. The up-sample ⊕ adds a zero between every second samples of input vector. The high- and low-pass filters $\tilde{g}$ and $\tilde{h}$ of

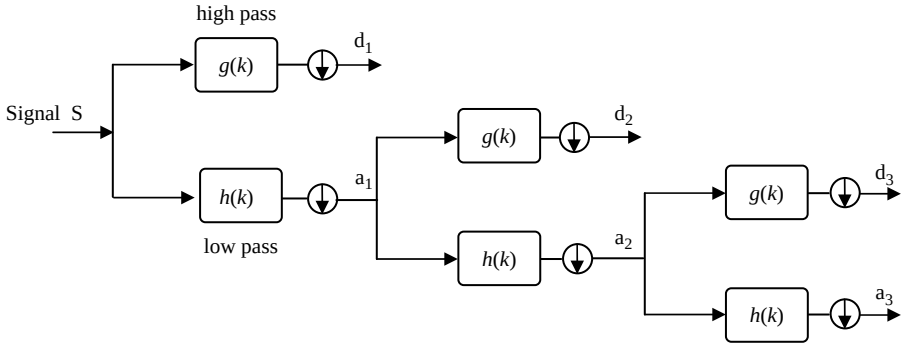

Figure 3.
Block diagram of signal decomposition in standard two channel multi resolution filter bank structure of DWT for three levels
($S = a_3 + d_3 + d_2 + d_1$)

the reconstruction are to satisfy the following relations required for perfect reconstruction of a signal:

$$h(k) = (-1)^k \tilde{h}(k) \tag{5}$$

$$g(k) = (-1)^k \tilde{g}(k) \tag{6}$$

3. Wavelet-based noise reduction

Noise reduction by wavelets as proposed by Donoho and Johnstone (1991) and Donoho (1993) and referred to as denoising, is distinctly different from other noise reduction approaches such as high-frequency filtering of signal components. Noise reduction by wavelets is based on the property of wavelet transform referred to as sparsity of signal representation in coefficient domain. Sparsity refers to clustering of coefficients into two groups of:

(1) a few large amplitude coefficients; and

(2) a large number of small valued coefficients.

Small amplitude coefficients are attributed to noise content of the signal. Noise reduction by wavelets deals with manipulation of wavelet coefficients in which coefficients below a judiciously selected threshold level are replaced by zero and inverse transform of manipulated (modified) coefficients is used to recover denoised signal; hence, noise is cleaned from the signal. Two approaches can be considered for tresholding:

3.1 Hard thresholding

In hard thresholding, only wavelet coefficients with absolute values below or at the threshold level are affected only, they are replaced by zero while others are kept unchanged. Modification of coefficients w in hard thresholding can be described as follows:

$$w_m = w \quad \text{if} \quad |w| \geq th \tag{7}$$

$$w_m = 0 \quad \text{if} \quad |w| < th \tag{8}$$

3.2 Soft thresholding

In soft thresholding, coefficients above threshold level are also modified where they are reduced by the amount of threshold:

$$w_m = \text{sign}(w)(|w| - th) \quad \text{if} \quad |w| \geq th \tag{9}$$

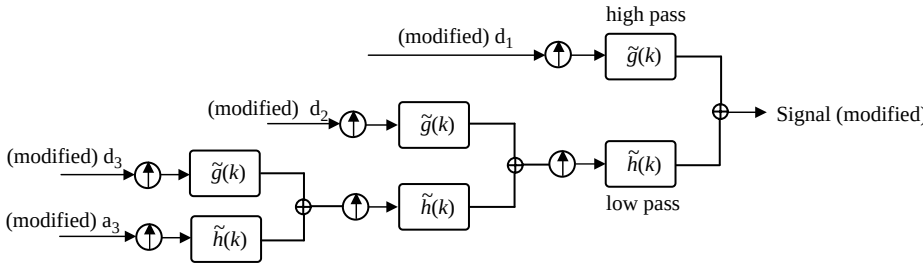

Figure 4.
Three level synthesis block diagram

$$w_m = 0 \quad \text{if } |w| < th \tag{10}$$

Donoho refers to soft thresholding as "shrinkage" where reduction in coefficient amplitudes by soft thresholding results in a reduction of the signal amplitude thus a "shrinkage" (Donoho and Johnstone, 1991, 1995).

For both of soft and hard thresholding, the following noise model is superimposed on the signal:

$$\hat{S}(i) = S(i) + n(i), \quad i = 1, \ldots, N \tag{11}$$

where an additive noise model is assumed. The quantity $S(i)$ is true signal and $n(i)$ indicates additive noise content of the signal. Under an orthogonal decomposition, linearity of wavelet transformation insures an additive noise model be also valid at the transform domain, i.e.:

$$\mathbf{W} = \mathbf{V} + \mathbf{U} \tag{12}$$

where, $\mathbf{W}$ is the vector of the empirical wavelet coefficients, while $\mathbf{V}$ and $\mathbf{U}$, indicate uncorrupted wavelet coefficients and noise content of $\mathbf{W}$, respectively. Vectors $\mathbf{W}$, $\mathbf{V}$ and $\mathbf{U}$ all have a length L. Vectors $\mathbf{V}$ and $\mathbf{U}$ can be considered as a realization of the coefficients of the true signal $S(i)$ and noise content $n(i)$, respectively. The object of noise modeling for noise reduction is to identify a suitable probability distribution for $\mathbf{U}$ and a suitable criteria for estimating noise level using empirical coefficients $\mathbf{W}$. This is treated as an statistical estimation problem that may be studied by superimposing a'priori probability distribution on $\mathbf{U}$ (Bayesian approach), or by a regression type model imposed on the noise components of the coefficients $\mathbf{U}$. The knowledge of statistical properties of the noise components are then used to determine a suitable threshold level for denoising and signal recovery (Donoho and Johnstone, 1995). Reconstruction of the signal is aimed to achieve a "best" estimate of the true signal in an attempt to reconstruct a replica of the true (noise free) signal. A schematic diagram of denoising process is shown in the Figure 5.

Donoho uses the coefficients at the highest detail level to arrive at a threshold level. Under this approach, it is assumed that coefficients at the highest frequency details d_1 of DWT, provide a good estimate of the noise content of the signal. A white noise model is superimposed on the coefficients where wavelet coefficients are assumed to be independently identically distributed (i.i.d.) random variables at the finest detail level. i.i.d random variables refer to the outcome of an experiment where each outcome is statistically independent of others and all belong to the same underlying probability density function. Under the assumption of i.i.d. for the wavelet coefficients and Gaussian white noise, one can show (Donoho and Johnstone, 1991, 1995) that under soft thresholding, the actual error in estimating the true signal is within $\log(n)$ factor of the ideal estimate under which the error is minimal (Donoho, 1995). Under this approach,

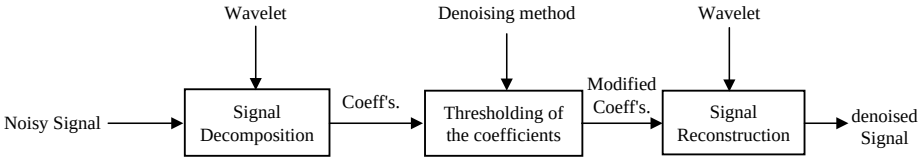

Figure 5.
Schematic diagram of denoising process

an estimate of the standard deviation of the coefficients in d_1 section is used to arrive at a suitable threshold for coefficient thresholding at all scales. This approach is global thresholding where the same threshold is applied on detail coefficients at all levels. Global thresholding is the most common approach used for denoising, it is also referred to as "universal thresholding." It can be shown that median absolute deviation (MAD) is a robust estimate of the standard deviation σ. Donoho and Johnstone(1991, 1995) use the following threshold for minimizing the max error in estimating the true signal:

$$Th = \sigma\sqrt{2\log n}, \quad \sigma = \frac{\text{MAD}}{0.6745} \tag{13}$$

MAD is median absolute deviation of the coefficients, i.e. MAD = Median ($|c|$)/0.6745, where **c** is the vector of the coefficients at highest frequency band d_1, and n is the coefficient length. For a scale dependent thresholding, each scale is treated separately but the same rule is applied on each scale to arrive at a threshold. Scalar 0.6745 in equation (13) is derived from statistical relationship between standard deviation σ and MAD for Gaussian distribution.

4. Inverse heat conduction problem

In this study, we consider inverse estimation of space and time varying heat flux on the surface of a 2D plate (Figure 6(a)). The unknown heat flux is discretized into n_s space components (Figure 6(b)). The heat conduction equation is written as:

$$\frac{\partial^2 T}{\partial x^2} + \frac{\partial^2 T}{\partial y^2} = \frac{1}{\alpha}\frac{\partial T}{\partial t} \tag{14a}$$

$$\left.\frac{\partial T}{\partial y}\right|_{(1)} = \left.\frac{\partial T}{\partial x}\right|_{(2)} = \left.\frac{\partial T}{\partial x}\right|_{(4)} = 0 \tag{14b}$$

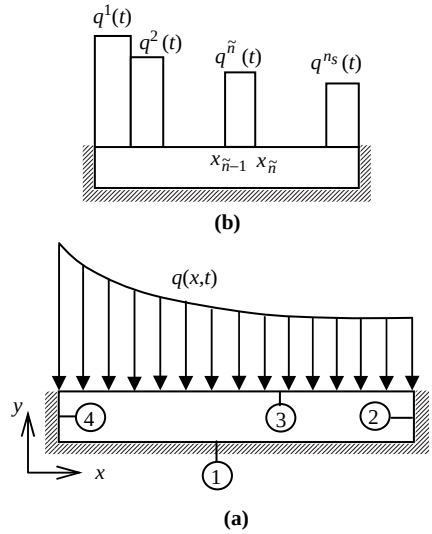

Figure 6.
(a) Inverse problem geometry; (b) decomposition of heat flux into n_s spatial components

$$k\frac{\partial T}{\partial y}\bigg|_{(3)} = q(x,t) \tag{14c}$$

$$T(x,y,t=0) = T_0 \tag{14d}$$

Each of the spatial components of flux (Figure 6(b)) is now assumed to be composed of M discrete time-wise subcomponent as shown in Figure 7. All of these time and space components are gathered in one vector $\vec{\mathrm{q}}$ as:

$$\begin{aligned}\vec{\mathrm{q}}_{n\times 1} &= \left[\, q^1(t_1) \quad q^1(t_2) \quad \ldots \quad q^1(t_M) \quad q^2(t_1) \quad q^2(t_2) \quad \ldots \quad q^2(t_M) \quad \ldots \,\right]^{\mathrm{T}} \\ &= \left[\, q_1^1 \quad q_2^1 \quad \ldots \quad q_M^1 \quad q_1^2 \quad q_2^2 \quad \ldots \quad q_M^2 \quad \ldots \,\right]^{\mathrm{T}}\end{aligned} \tag{15}$$

superscript T denotes the transpose sign, $n = n_{\mathrm{s}} \times M$ is total number of the unknowns and $\vec{\mathrm{q}}$ is the vector of unknown heat fluxes. Pulse sensitivity coefficient with respect to each component of vector $\vec{\mathrm{q}}$ is defined as:

$$X\left(x_k, y_k, t_m, q_{\tilde{m}}^{\tilde{n}}\right) = \frac{\partial T(x_k, y_k, t_m)}{\partial q_{\tilde{m}}^{\tilde{n}}} \quad \text{for} \begin{cases} \tilde{m} = 1, 2, \ldots, M \\ \tilde{n} = 1, 2, \ldots, n_s \end{cases} \tag{16}$$

subscript k indicates the index number of each sensor ($k = 1,2\ldots,K$). Sensitivity coefficients will be used later in the development of the inverse algorithm. Governing equation for these coefficients are obtained by taking the derivative from heat equation (14a)-(14d) with respect to each $q_{\tilde{m}}^{\tilde{n}}$:

$$\frac{\partial^2 X}{\partial x^2} + \frac{\partial^2 X}{\partial y^2} = \frac{1}{\alpha}\,\frac{\partial X}{\partial t} \tag{17a}$$

$$\frac{\partial X}{\partial y}\bigg|_{(1)} = \frac{\partial X}{\partial x}\bigg|_{(2)} = \frac{\partial X}{\partial x}\bigg|_{(4)} = 0 \tag{17b}$$

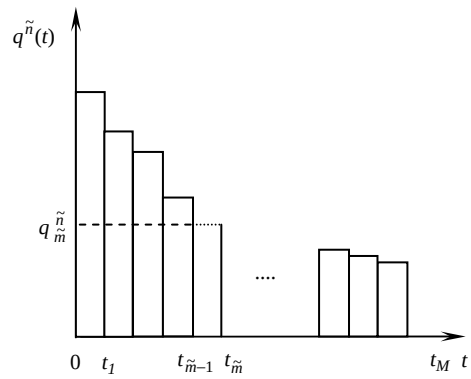

Figure 7.
Discretization of each spatial component of heat flux ($\tilde{n} = 1, 2, \ldots, n_{\mathrm{s}}$) into M time steps ($\tilde{m} = 1, 2, \ldots, M$)

$$k\frac{\partial X}{\partial n}=\begin{cases}\begin{cases}1 & (t_{\tilde{m}-1}<t\le t_{\tilde{m}})\\ 0 & \text{other } t\end{cases}; & \text{for } x_{\tilde{n}-1}<x<x_{\tilde{n}};\quad (\tilde{n}=1,2,\ldots,n_s)\\ 0 & \text{elsewhere}\end{cases} \tag{17c}$$

$$X(x,y,t\le t_{\tilde{m}})=0\quad(\tilde{m}=1,2,\ldots,M) \tag{17d}$$

The equations (17a)-(17d) should be solved "$M\times n_s$" times (for $\tilde{m}=1,2,\ldots,M$ and $\tilde{n}=1,2,\ldots,n_s$) to compute $X(x,y,t,q^{\tilde{n}}_{\tilde{m}})$. In order to obtain the unknowns vector $\vec{q}$, a sum of square error function, which must be minimized, is now defined as:

$$f=\sum_{k=1}^{K}\sum_{m=1}^{M}[Y(x_k,y_k,t_m)-T(x_k,y_k,t_m,\vec{q})]^2 \tag{18}$$

where, K is total number of sensors, Y is the measured temperature at sensor location of (x_k, y_K), and T is the computed temperature utilizing the direct heat conduction model (equation (14a)-(14d)) with an assumed or given vector for $\vec{q}$. In fact, f is the objective function of the problem and is an implicit function of its variable $\vec{q}$. The design vector $\vec{q}$ should be found in a manner that minimizes the objective function f. The problem of estimating the vector $\vec{q}$ which minimizes f can be considered as a non-linear programming (optimization) problem.

The conjugate gradient method (CGM) and the VMM both belong to unconstrained optimization techniques. A survey of existing works in whole domain IHCP reveals that CGM has been used so far as the tool for minimizing of the object function f in inverse problems. The textbook by Ozisic and Orlande (2000) and the book by Alifanov (1994) give a comprehensive discussion of CGM accompanied by IHCP. Moreover, many technical papers have been published on the subject of CGM in inverse problems. For example, Huang and Chen (2000), Chen *et al.* (2001), Linhua *et al.* (1999), Prud'homme and Nguyen (2001), Louahlia-Gualous *et al.* (2003), Singh and Tanaka (2001) and Machado and Orlande (1997), all have used CGM in various inverse heat transfer problems. However, VMM is more powerful than CGM in non-linear unconstrained programming (Rao, 1995). The VMM is very stable and continues to progress towards the minimum even when dealing with highly distorted and eccentric functions. The authors Kowsary *et al.* (2006) and Pourshaghaghy *et al.* (2007) have recently applied the VMM successfully for solving IHCP. The VMM is also utilized in this paper to minimize the function of squares errors. The detailed iterative procedure of VMM for finding vector of unknowns $\vec{q}$ can be found in aforementioned references.

In whole domain type of IHCP, some oscillations may appear in the estimated solutions near the final times such that the estimated heat flux at a few time steps near final times is discarded (Beck *et al.*, 1985; Huang and Chen, 2000). In what follows, an approach is given to obtain more accurate solution near final times and avoid such instabilities. In this approach, a greater final time with respect to the desired domain is considered but the unknowns are estimated only inside the small time domain (desired time) using sensor data in the entire time domain. That is, the total number of time steps M is divided into M_1+M_2 time steps where additional time steps M_2 is much less than M_1 and are taken to damp the instabilities. Then, the estimation of heat flux is

performed only for M_1 time steps using $M_1 + M_2$ sensor data. The value of M_2 should be chosen such that the temperature at the sensor locations are affected by the final heat flux component. An approximate value can be inferred from the "penetration depth" concept. In each iteration, the value of unknowns inside M_2 time domain (used in equation (14a)-(14d) for calculating T) is considered to be equal to their value at the end of the main M_1 time domain and there is no need to any information about real end fluxes. The number of search variables (components of $\vec{q}$) is $n = M_1 \times n_S$. The sensitivity coefficient equation (equation (17a)-(17d)) should be solved in total domain of $M = M_1 + M_2$. The objective function and its gradients are also calculated in total time domain M; i.e. M in equation (18) is equal to $M_1 + M_2$.

In the case of non-noisy data, either of the following criteria can be used to terminate the iterative process of VMM:

$$|f| \leq \varepsilon \tag{19}$$

$$\|\vec{\nabla} f\| \leq \varepsilon \tag{20}$$

In this work, $\|\vec{\nabla} f\| \leq \varepsilon$ is used as the stopping criteria, where ε is an arbitrary small number. In the case of noisy data, however, ε should be chosen based on iterative regularization criteria (discrepancy principle) in order to reduce sensitivity of the solution to the random noise errors. The main idea in iterative regularization is to stop the iterative procedure close to but not at the optimum point. This will, then, tend to regularize the solution and to damp the effects of random noises in data. Stopping criteria in iterative regularization for a constant value of noise amplitude is given by Ozisic and Orlande (2000):

$$|f| \leq K \times M \times A^2 \tag{21}$$

where, K and A are total number of sensors and noise amplitude, respectively, and M is the total number of time steps. If M is divided into M_1 and M_2 as described previously, M_1 should be used in equation (21) instead of M.

5. Results and discussion

Let's consider the upper surface of slab in Figures 6(b) being exposed to five unknown heat flux space components ($n_s = 5$) each one with time varying forming a vector as described in Section 4. The slab is made of aluminum (thermal diffusivity of 9.71×10^{-5} m/s) with the dimensions of 10×1 cm having an initial temperature of 300 K. The thermal properties are assumed to be temperature independent. Temperature dependent properties will have no bearing on the idea proposed in this paper. The direct heat conduction calculations implemented in the inverse scheme were performed using an ADI finite difference method (Anderson *et al.*, 1984). Five space components of heat flux are estimated in a total time equal to 28 s. An additional sensor data for 2 s were used after final time in order to stabilize near end solutions as described in previous section. To simulate sensor temperatures, the top surface of the slab was numerically exposed to a known five component convective heat transfer coefficient and known fluid temperature. The fluid temperature is considered to be 500 K. The upper surface of the plate was divided into five equal-sized sections. In accordance with thermal boundary layer growth, the convective coefficients in each section were chosen to be decreasing from left to right of the plate as: 1,000, 800, 600,

400, and 200 W/m^2 K. Five sensors were assumed to be located at (1, 0.8), (3, 0.8), (5, 0.8), (7, 0.8) and (9, 0.8) cm with respect to the coordinate system shown in Figure 6. Then, temperature values were obtained using the direct heat conduction calculations and their values at sensor locations were saved and used as sensor data. Time step for the inverse procedure and numerical ADI calculations were different from each other. Time step in all direct calculations was 0.01 s while the calculated temperatures at sensor locations were saved every 0.1 s in order to be used in inverse procedure. This value of time step (10 samples per second) precludes random error correlation in most real situations.

Figure 8 shows five estimated components of heat flux using VMM and non-noisy sensor data. Stopping criteria was chosen as $\|\nabla f\| \leq 2 \times 10^{-3}$, and an initial value equal to unity was used for all unknowns. Comparison of the real and the estimated fluxes in this figure indicates the accuracy of the proposed inverse method. The bias seen in the estimated heat flux near the end of time domain is common in all whole domain IHCP solutions, although using the M_2 additional data (as described previously) has reduced this undesired effects greatly.

At the next step, noise was added to the sensor data using the following equation:

$$\hat{T} = T + \omega A \tag{22}$$

in which $\hat{T}$ is noisy temperature and T is non-noisy temperature, ω is a normally distributed random number within -2.576 to 2.576 for a 99 percent confidence bound. A is the standard deviation of the measurements which was set equal to 1.2 K (i.e. 1 percent of maximum temperature rise). A plot of the simulated temperatures at the sensor locations is shown in Figure 9. Heat fluxes estimated from these noisy data with applying the iterative regularization method are shown in Figure 10.

In the last stage, the same noisy data used as above, were denoised by wavelet denoising algorithm described earlier. In this paper, data simulation and computations

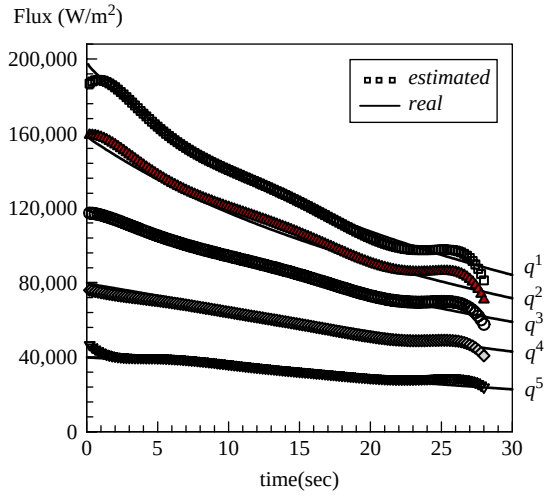

Figure 8.
Actual and estimated heat fluxes using non-noising temperature data

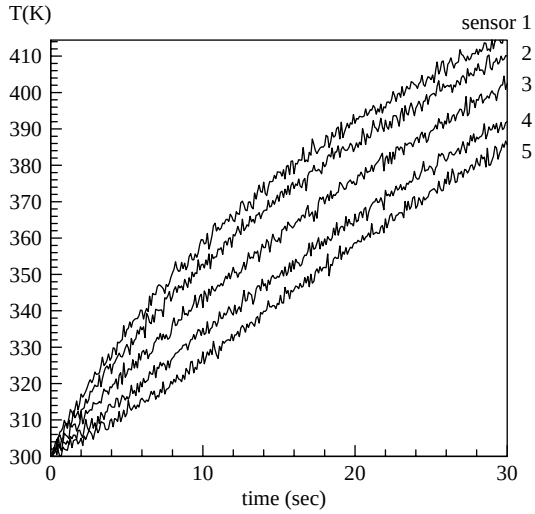

Figure 9.
Simulated noisy temperature for the each of the five sensors

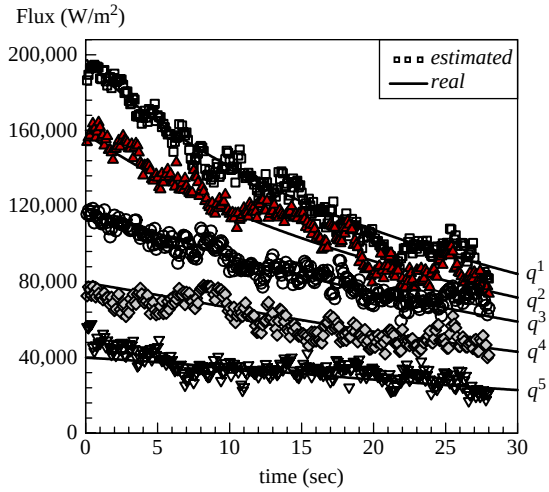

Figure 10.
Estimated heat fluxes using noisy data with iterative regularization

of direct and inverse heat conduction were carried out using FORTRAN; while for wavelets calculations and denoising, the wave-menu of MATLAB toolbox was used. Computational load of denoising by MATLAB is not a significant issue. MATLAB uses seven different criteria for thresholding where they can be implemented in either soft or hard thresholding. In our data analysis, we used a conservative thresholding criteria referred to as "penalize high" in MATLAB. Based on the results of several trials and observing the "edge effects" it was found that hard thresholding often gave better results as compared with those of soft thresholding. The edge effect refers to oscillations at the initial or final regions of the reconstructed signal. These oscillations in hard thresholding were found to be less than those of soft thresholding. We used coif-2 for

analyzing wavelet in a multi resolution structure with eight levels for decomposition. It was found that factors contributing to an improved noise separation include:

- wavelets having short support length;
- high-decomposition levels; and
- the length of the original signal to be of large value.

Figure 11 shows decomposition of first sensor data into eight levels in standard multi-resolution pyramid. In this figure, "*S*" is original noisy signal of 300 sample length with noise amplitude of 1.2 K. As can be shown in this figure, a large percentage of noise content of the signal resides in d_1 and d_2. This is mainly due to the fact that the frequency of noise components of the signal lies often in high-frequency band as compared with frequency of the signal. It should also be noted that the coefficients at d_1 are of low amplitudes as compared with those of the other levels, and as such these coefficients belong mostly to noise content of the signal. After analyzing the signal, denoising is performed on the signal components as shown in Figure 12. Threshold level for d_1 is shown by dotted line and as seen, almost all of signal components in d_1 as well as d_2 and d_4 are set to zero.

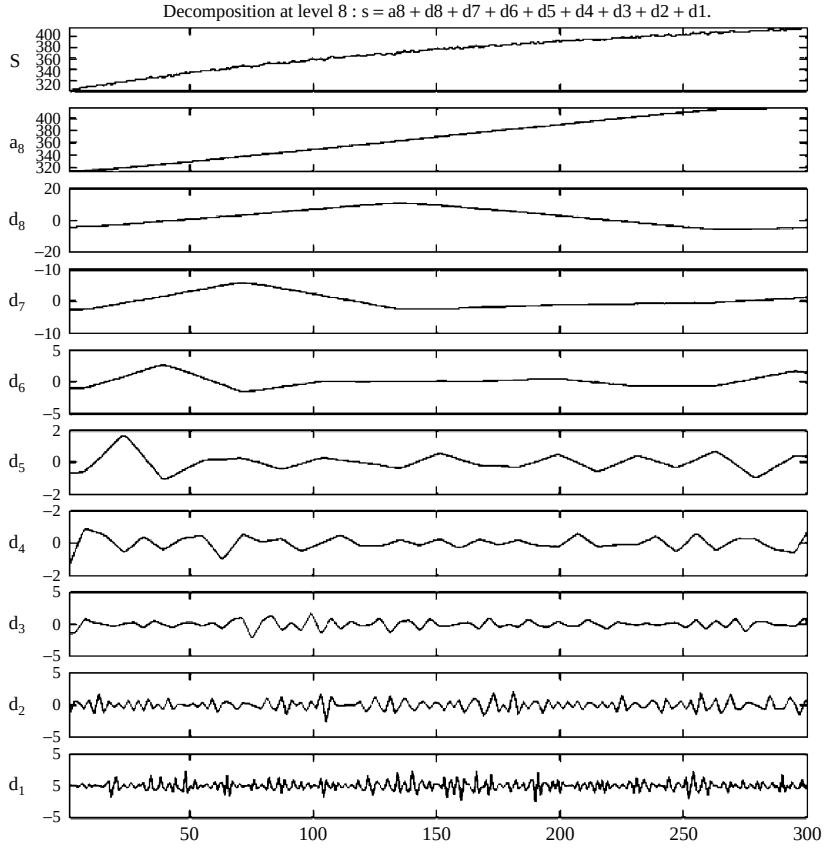

Figure 11.
Decomposition of one of sensor data (signal *S*) into eight levels of filter blank structure

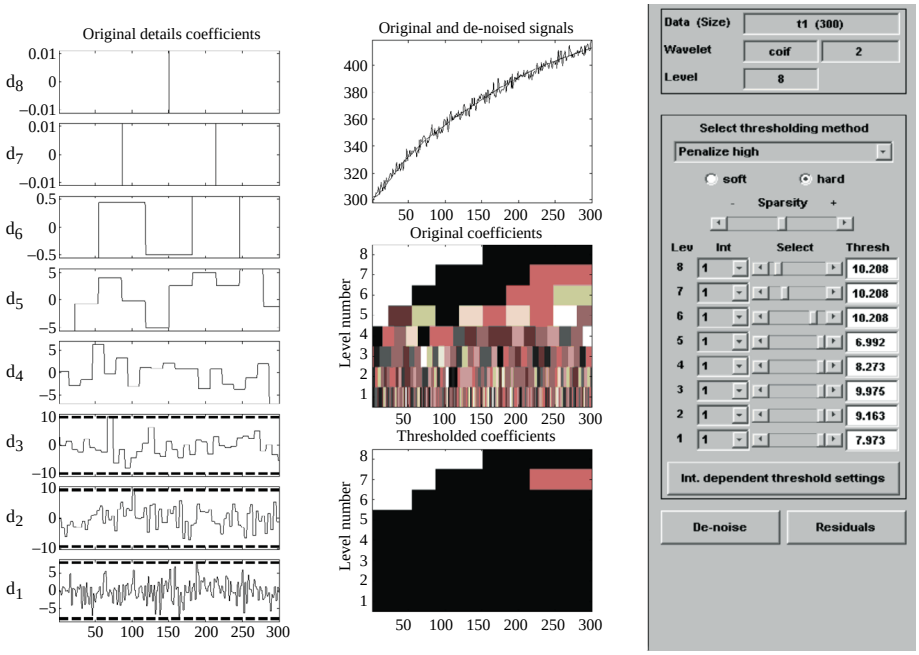

Figure 12.
Illustration of computed thresholds in denoising stage

In Figure 12, the midsection indicates original signal (top) and the coefficient of original and denoised signal (mid and lower) at different levels. Coefficient amplitude is indicated by the brightness of the gray-scale, where black color corresponds to zero coefficient value.

Noisy and final denoised signals of five sensors are compared as shown in Figure 13. In this figure, the difference between noisy and non-noise original data ($T_{\text{noisy}} - T$) is compared with the difference of denoised and original data ($T_{\text{denoised}} - T$). The "edge effect" as a shortcoming of wavelet transform is observed at the initial and end of each signal. The more length of the original signal not only contributes to the less edge effects but also the more accurate thresholding could be achieved.

Figure 14 shows heat fluxes as estimated by denoised data but without iterative regularization. A comparison between Figures 8-14 show that applying wavelet algorithm for noise reduction of data has appreciable effects on IHCP results. A root mean square error percentage, e_{RMS}, is defined to compute the difference between estimated and true values of components of vector $\vec{q}$ as:

$$e_{\text{RMS},\ \vec{q}} = \left(\sqrt{\frac{1}{M_1 \times n_s} \sum_{\tilde{n}=1}^{n_s} \sum_{\tilde{m}=1}^{M_1} \left(1 - \frac{q^{\tilde{n}}_{\text{est.},\tilde{m}}}{q^{\tilde{n}}_{\text{real},\tilde{m}}} \right)^2} \right) \times 100 \tag{23}$$

Table I gives the errors of IHCP solutions related to Figures 8-14. This table confirms once again the capability of proposed denoising algorithm noting that the

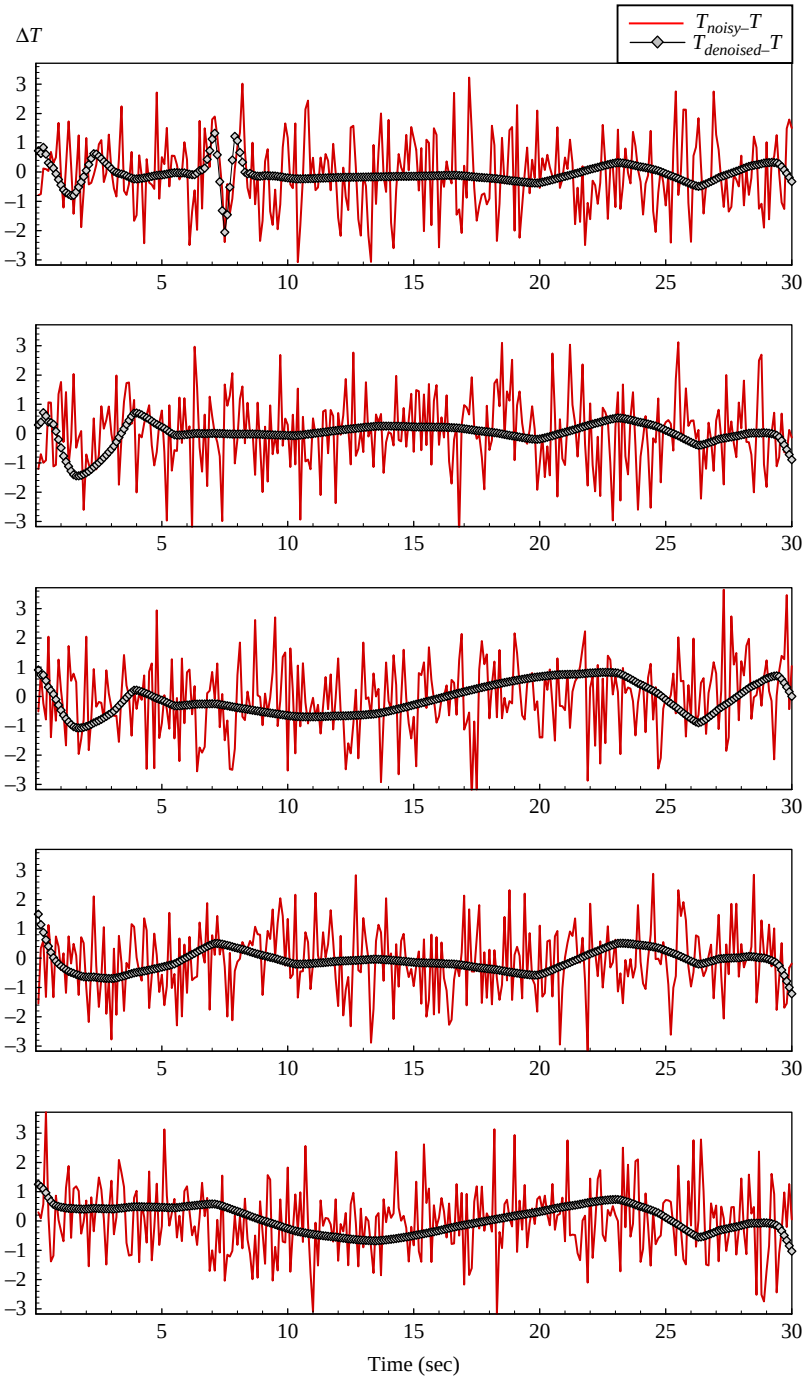

Figure 13.
Comparison between the difference of noisy and non-noisy data with difference of denoised and non-noisy data, for five sensors

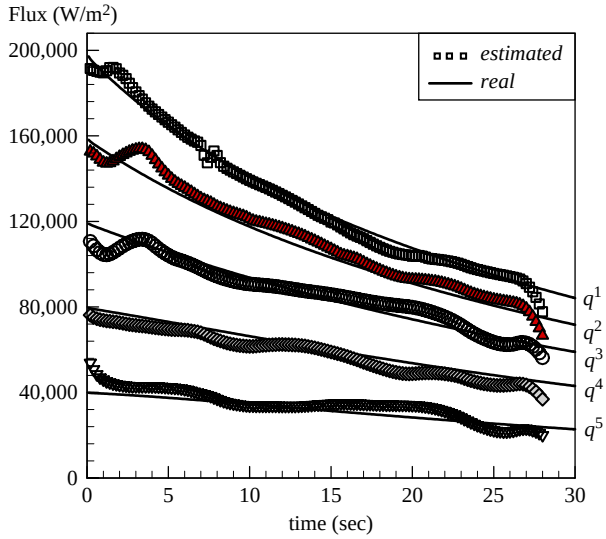

Figure 14.
Estimated heat fluxes using denoised data

		$e_{RMS,\tilde{q}}$ (percent)	Number of the VMM iterations
Table I. Error percentage in prediction of flux	Using non-noisy data (Figure 8)	3.99	57
	Noisy data with regularization (Figure 10)	9.69	39
	Using denoised data (Figure 14)	7.21	30

errors when using denoising is lower, as much as 25.6 (percent) than those of iterative regularization.

6. Conclusion

Potential use of wavelets for noise reduction was successfully tested to improve IHCP results. The VMM was utilized as minimization tool in whole domain inverse problem instead of the CGM. Denoising by wavelets provides a considerable advantage due to its low-computational load during its implementation using wavemenu of MATLAB. Although the iterative regularization is also considered a simple method for decreasing sensitivity to the noise errors in whole domain IHCP, the method presented in this work not only yields accurate results in whole domain procedure, but also it will be worth to be applied in sequential methods of IHCP where iterative regularization is not applicable.

References

Al-Khalidy, N. (1998), "On the solution of parabolic and hyperbolic inverse heat conduction problems", *International Journal of Heat and Mass Transfer*, Vol. 41, pp. 3731-40.

Alifanov, O.M. (1994), *Inverse Heat Transfer Problems*, Springer-Verlag, Berlin.

Anderson, D.A., Tannehill, J.C. and Pletcher, R.H. (1984), *Computational Fluid Mechanics and Heat Transfer*, Hemisphere Publishing Corp., Warsaw.

Beck, J.V., Blackwell, B. and Clair, C.R. (1985), *Inverse Heat Conduction*, Wiley, New York, NY.

Burrus, C.S., Guo, H. and Gopinath, R.A. (1997), *Introduction To Wavelets & Wavelet Transforms: A Primer*, Prentice-Hall, Englewood Cliffs, NJ.

Chen, U.C., Chang, W.J. and Hsu, J.C. (2001), "Two-dimensional inverse problem in estimating heat flux of pin fins", *International Communications in Heat and Mass Transfer*, Vol. 28 No. 6, pp. 793-801.

Donoho, L.D. (1993), "Nonlinear wavelet methods for recovery of signals, densities, and spectra from indirect and noisy data", *Different Perspectives on Wavelets, Proceeding of Symposia in Applied Mathematics*, Vol. 47, Amer. Math. Soc., Providence, RI, pp. 173-205.

Donoho, L.D. (1995), "Denoising by soft thresholding", *IEEE Trans on Information Theory*, Vol. 41 No. 3, pp. 613-27.

Donoho, L.D. and Johnstone, I.M. (1991), *Minimax Estimation via Wavelet Shrinkage*, Dept of Statistics, Stanford University, Stanford, CA.

Donoho, L.D. and Johnstone, I.M. (1995), "Adapting to unknown smoothness via wavelet shrinkage", *Journal of American Stat. Assoc.*, Vol. 90, pp. 1200-24.

Huang, C.H. and Chen, W.C. (2000), "A three dimensional inverse forced convection problem in estimating surface heat flux by conjugate gradient method", *International Journal of Heat and Mass Transfer*, Vol. 43, pp. 3171-81.

Ji, C. and Jang, H. (1998), "Experimental investigation in inverse heat conduction problem", *Numerical Heat Transfer, Part A*, Vol. 34, pp. 75-91.

Kalman, R.E. (1960), "A new approach to linear filtering and prediction problems", *ASME Journal Basic Eng.*, pp. 35-45, Ser. 82d.

Kowsary, F., Behbahaninia, A. and Pourshaghaghy, A. (2006), "Transient heat flux function estimation utilizing the variable metric method", *International Communications in Heat and Mass Transfer*, Vol. 33 No. 6, pp. 800-10.

Linhua, L., Heping, T. and Qizheng, Y. (1999), "Inverse radiation problem of temperature field in three-dimensional rectangular furnace", *International Communications Heat and Mass Transfer*, Vol. 26 No. 2, pp. 239-48.

Louahlia-Gualous, H., Panday, P.K. and Artioukhine, E.A. (2003), "Inverse determination of the local heat transfer coefficients for nucleate boiling on a horizontal cylinder", *ASME Journal of Heat Transfer*, Vol. 125, pp. 1087-95.

Machado, H.A. and Orlande, H.R.B. (1997), "Inverse analysis for estimating the timewise and spacewise variation of the wall heat flux in a parallel plate channel", *International Journal for Numerical Methods for Heat & Fluid Flow*, Vol. 7 No. 7, pp. 696-710.

Mallat, S. (1989), "A theory for multiresolution signal decomposition: the wavelet representation", *IEEE Pattern Anal. and Machine Intell.*, Vol. 11 No. 7, pp. 674-93.

Ozisic, M.N. and Orlande, H.R.B. (2000), *Inverse Heat Transfer, Fundamentals and Applications*, Taylor & Francis, New York, NY.

Pourshaghaghy, A., Kowsary, F. and Behbahaninia, A. (2007), "Comparison of four different versions of the variable metric method for solving inverse heat conduction problems", *Heat and Mass Transfer*, Vol. 43 No. 3, pp. 285-94.

Prud'homme, M. and Nguyen, T.H. (2001), "Solution of inverse free convection problems by conjugate gradient method: effects of Rayleigh number", *International Journal of Heat and Mass Transfer*, Vol. 44, pp. 2011-27.

Rao, S.S. (1995), *Optimization, Theory and Applications*, 2nd ed., New Age International (P) Limited Publishers, New Delhi, 9th reprint.

Singh, K.M. and Tanaka, M. (2001), "Dual reciprocity boundary element analysis of inverse heat conduction problems", *Computer Methods in Applied Mechanics and Engineering*, Vol. 190, pp. 5283-95.

Strang, G. and Nguyen, T. (1996), *Wavelets and Filter Banks*, Wellesley-Cambridge Press, Wellesley, MA.

Tuan, P. and Ju, M.C. (2000), "The validation of the robust input estimation approach to two dimensional inverse heat conduction problems", *Numerical Heat Transfer, Part B*, Vol. 37, pp. 247-65.

Tuan, P., Ji, C., Fong, L. and Huang, W. (1996), "An input estimation to on-line two dimensional inverse heat conduction problems", *Numerical Heat Transfer, Part B*, Vol. 29, pp. 345-63.

Woodbury, K.A. (2003), *Inverse Engineering Handbook*, CRC Press, Boca Raton, FL.

Corresponding author
F. Kowsary can be contacted at: fkowsari@ut.ac.ir